Kinetic study of Fischer–Tropsch reaction over Iron Nano Catalysts in slurry reactor

IOP Conf. Series: Journal of Physics: Conf. Series **1294** (2019) 052027 doi:10.1088/1742-6596/1294/5/052027

Kinetic study of Fischer–Tropsch reaction over Iron Nano Catalysts in slurry reactor

Abdulqadier Hussien Al khazraji and Ziad T I Alkayar

Department of Chemistry, College of Education for Pure Science, University of Diyala, Iraq

E-mail: ahnhkm@yahoo.com

Abstract. The common belief is that water can affect the performance of iron nanocatalysts (FT) in Fischer-Tropsch reaction by reducing the activity, selectivity and the rate of reaction. In this study, using nano iron - Paraffin/ polymer matrix as nanocatalysts have enhanced the FTS performance in the presenceof water partial pressure.Thermal decomposition method was successfully used to synthesize iron nanoparticles with different nano size, which measured using scattering of dynamic light. In the Fe - Paraffin/ polymer (Fe-P/p) systemsthe polymers;polyethylene glycol (PEG) and styrene butadiene rubber (SBR)were used. The conversion of the synthesis gas which depends on the contact time wasfrom 4% to 74%.XRD and AFM confirmed that there are two forms of iron;Fe_3O_4 and δ-FeOOH. The high rateof reaction of FTS (R_{CO}) was observed in the Fe–paraffin– PEG as nanocatalyst. The experimental data was used to analyze the kinetic models for the flow of CO;this gave water partial pressure(P_{H2O}),kinetic and thermodynamic characteristics of the process.The relationship between the values of the activation energies and the polymers nature of the stabilizers were established.

Keywords: Fischer-Tropsch synthesis, nanocomposite iron oxide catalysts, polymer, slurry reactor.

I. Introduction

Due to the highly catalytic effect such as activity, stability and selectivity in Fischer Tropsch synthesis (FTS), nano iron catalysts-paraffin/polymer system are widely used in many studies.[1-5]Since during long-term operation in the reaction medium with high temperatures the other catalytic systems undergo agglomerating leading to decrease activity, and this because of decreasing the disparity of the particles of the active component.[6]Therefore, the development of catalysts to change the dispersion of the active component and study the agglomerating mechanisms increased the service life of catalysts.[7]The control of changes in the size particles led to activate the component of catalysts.[8]The development of the Fischer-Tropsch synthesis devices like stationary layer and slurry layer have solved a number of technological problems. Therefore, modern technologies have a slurry reactor with a nano-sized catalyst.[9]The optimum metal content of classical catalysts for three-phase Fischer Tropsch synthesis (FTS) is 20%.[10]Since the nano-scale suspensions easily agglomerate,[11] polymer systems as a stabilizer

wasused to overcome the issue.[1]Botes and co-workers have studied theinfluenceofwater partial pressure on the Fischer−Tropsch synthesis (FTS).They have reported that water has negligible effect on the overall FT reaction rate, but lower the methane selectivity and increases the CO_2 selectivity.[12]

The purpose of this paper is to determine the experimental rates of some catalysts in FT reactions using kinetic equations.

Ii. Experimental

A. Iron nano catalyst Preparation

Using thermal decomposition, Fe (6 gm)/ paraffin (100 mL) was added to polymer (10gm) in aqueous solution of $Fe(NO_3)_3 \bullet 9H_2O$. Iron nitrate solution was added dropwise to the paraffin/ polymer, stirred under inert gas at 280°C for 4hour.[1-5]

B. Fischer-Tropsch Reaction

The Fischer Tropsch synthesis (FTS) was carried out in the slurry reactor 250 mL. The iron nanoparticles dispersion in the paraffin/ polymer mixture was loaded into slurry reactor under a pressure reactor (20 atm), temperature 220 to 320 ºC.H_2:CO (1:1) molar feed ratiowas conducted under mechanical stirring (200 rpm) for 72 hour. The synthetic gas (H_2/ CO) was prepared by mixing H_2 and CO *via* two mass flow controllers, enabling the desired H_2/ CO ratio to be obtained.The results were listed in Table 1.

C. Catalysts Analysis

To determine the nanoparticles size, we used the means of scattering of dynamic light on a Malvern Zetasizer Nano ZS instrument (Table 2). The samples were analyzed using atomic force microscopy (AFM). All measurements were performed using the HybriD technique DMT model to determine the nanoparticles in the deep surface of the samples (Figure 2).The studies were doneusing Shimadzu XRD-7000 apparatus.The analysis provides information about the phase composition of iron and paraffin compounds in the samples. The Qualitative analysis was carried out according to the intensity of peaks and their position and the image of X-rays.

III. Results and discussion

A. Fischer-Tropsch Synthesis

As nanocatalysts were loaded initially in slurry reactor, flow synthetic gas was passed over it under the required conditions.Figure 1 shows that temperature is highly effected the CO conversion, yields of hydrocarbons and CO_2, and the selectivity of liquid hydrocarbon. The CO conversion (%) and selectivity (%) of liquid hydrocarbons (C_{5+}) are calculated using:

$$\text{CO conversion (\%)} = \frac{(\text{moles } CO_{in}) - (\text{moles } CO_{out})}{\text{moles } CO_{in}} \times 100$$

$$\text{Selectivity of j product (\%)} = \frac{\text{moles of j product}}{(\text{moles } CO_{in}) - (\text{moles } CO_{out})} \times 100$$

The distribution of the liquid products and gases of the Fischer-Tropsch synthesis presented as shown in Table 1 and Figure 1.

Table 1 Catalytic CO conversion and product selectivity under FTS conditionsof Fe- paraffin/polymer catalysts.

Systems Fe- P/ P	T°C	*A	*X_{CO}, %	*$Y_{H.C}$, g/m^3				S, %
				C_1	C_2-C_4	C_{5+}	CO_2	
Fe- P/ PEG	320	6	74.0	37.0	30.0	62.0	214.0	65.0
Fe- P/ SBR	300	5	66.0	37.0	31.0	60.0	190.0	54.0

*X_{CO}, % : CO conversion, %. *S,% : Product Selectivity, %.*A: Activity in mol CO g cat*10^{-6}
*$Y_{H.C}$: Yield of liquid hydrocarbons (C_{5+}) and gasses (C_1 ,CO_2 andC_2-C_4), gm/m^3.

Table 1 and Figure (1a,b) indicatesthattheCO conversion andthe yield of liquid hydrocarbons are almost same. The yield of CO_2that obtained using Fe -P/SBR nanocatalyst was low, while using Fe -P/ PEG gave higher yield of CO_2 conversion and better selectivity for liquid hydrocarbons. For the undesirable products gases (C_1 and C_2-C_4) both produced same yield (Figure1c and d).So, we think that the structure of the different polymers isthe reason for suchobtained results.

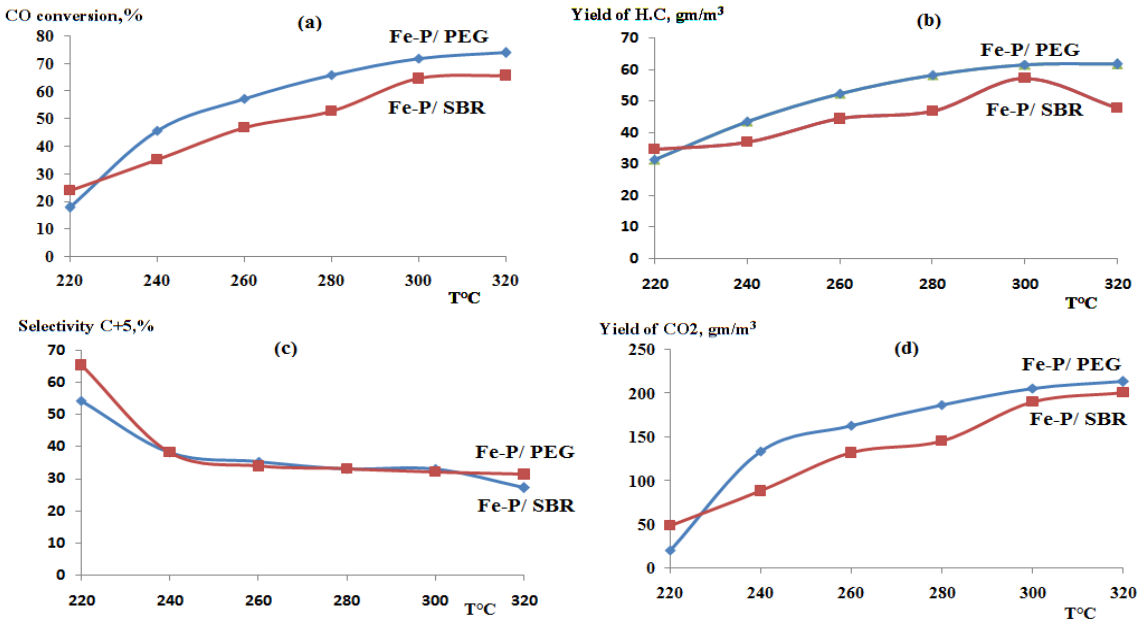

Fig. 1 Comparison of iron nano catalysts performance: (a) CO conversion, (b) yield of C_{5+}, (c) Selectivity of C5+ and (d) yield of CO_2 gas over Fe- P/ SBR and Fe- P/ PEG.

X-ray diffraction patterns of the prepared catalysts (Figure 2) show narrow and average intensity peaks, this would lead to suggest that the sample is good crystalline large particle sizes and theFe_3O_4 is the most abundant phase, beside the amorphous FeOOH. The following diffraction peaks are 2θ: 30°, 33°, 35°, 41°, 45° indicatingthatthe phase magnetite (Fe_3O_4) is present[5,13,14] and it is responsible for the effectiveness of nanocatalysts in the Fischer Tropsch synthesis.

The morphology of Fe - P/ P nanocatalysts were illustrated by AFM images and showed in (Figure 3 a and b). Although AFM revealed that the nanocatalyst with SBR as shown in (Figurer 3 b) have irregular surface with a littleconverging cliffs, this caused the stability of iron nanoparticles in the

paraffin/ polymer matrix. The distribution of nanoparticles in the polymer and paraffin with change the particle size and their stabilities in matrix are responsible for the effectiveness of the nanocatalyst. The high peak for Fe-P/ SBR is 33 nm, while for the catalyst Fe-P/ PEG the high peaks was 0.28 µm (280 nm). As a result, the presence of the large iron nanoparticles leads to form active catalysts Fe-p/ PEG.

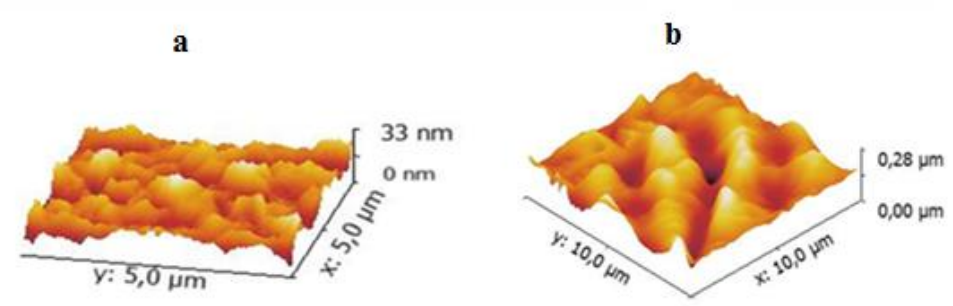

Fig.2 AFM images of a (a) Fe-P/ SBR and (b) Fe-P / PEG nanocatalysts

B. Particles size

The study of the samples using dynamic light scattering showed that the treatment of the suspension with Ar gas has a significant effect on the particle size of the suspension after preparation.From Table 2for all preparation times,adding polymers led to the formation of bimodal; small and large particle size. Distribution of nano iron suspension with PEGcontains 9%at 181 nm and 91% at 655 nm of the particles after 2 hour.Using SBR resulted in19% at 171 nmand 81% at 664 nm.However, the addition of SBR polymer into the composition of the catalyst suspension leads to a twofold increase in the small nanoparticles size from 9% to 19% as mentioned.Additionally, the light scattering intensity suggests that large particles (greater than 650nm) are dominant in the suspension, and the weight content of these particles is significantly higher than the fraction of nano iron particles with size less than 170 nm. This mean the nanocatalyst of large particles and higher weight content would give better results in the FTS see Table 2.

Table 2 The effect of the processing time under Ar gas on the suspension after ending addition of the precursor solution.

Nanocatalysts type	Changes in Particles size (nm) of catalyst system over time in hour					
	nm at 0* hour	Content,%	nm at 1* hour	Content,%	nm at 2* hours	Content,%
Fe-P/PEG	213	11	232	17	181	9
	779	89	804	83	655	91
Fe-P/SBR	145	7	134	11	171	19
	765	93	626	89	664	81

* Fe-P/PEG = Fe- paraffin/ polyethylene glycol.
* Fe-P/SBR = Fe- paraffin/ Styrene Butadiene rubber.
*0 hour :after the addition of last drop of iron solution under stirring and Ar gas.
*1 hour : After one hour with stirring under Ar gas.
*2 hour :After two hours with stirring under Ar gas.

C. H_2O partial pressure

Graphs from figure 4, clearly indicates the effect of the production of water on the parameter of Fischer Tropsch (CO conversion, yield of liquid hydrocarbons) and increasing the CO_2 partial pressure. This fact is expected due to the presence of polymer in the nanocatalyst structure, especially in the case of Polyethylene glycol (PEG) which contains OH groups.Thiswould lead to increase water releaseandincrease the reaction temperature from 220 to 320 °C. The process clearly generates an increase in the water partial pressure as well.

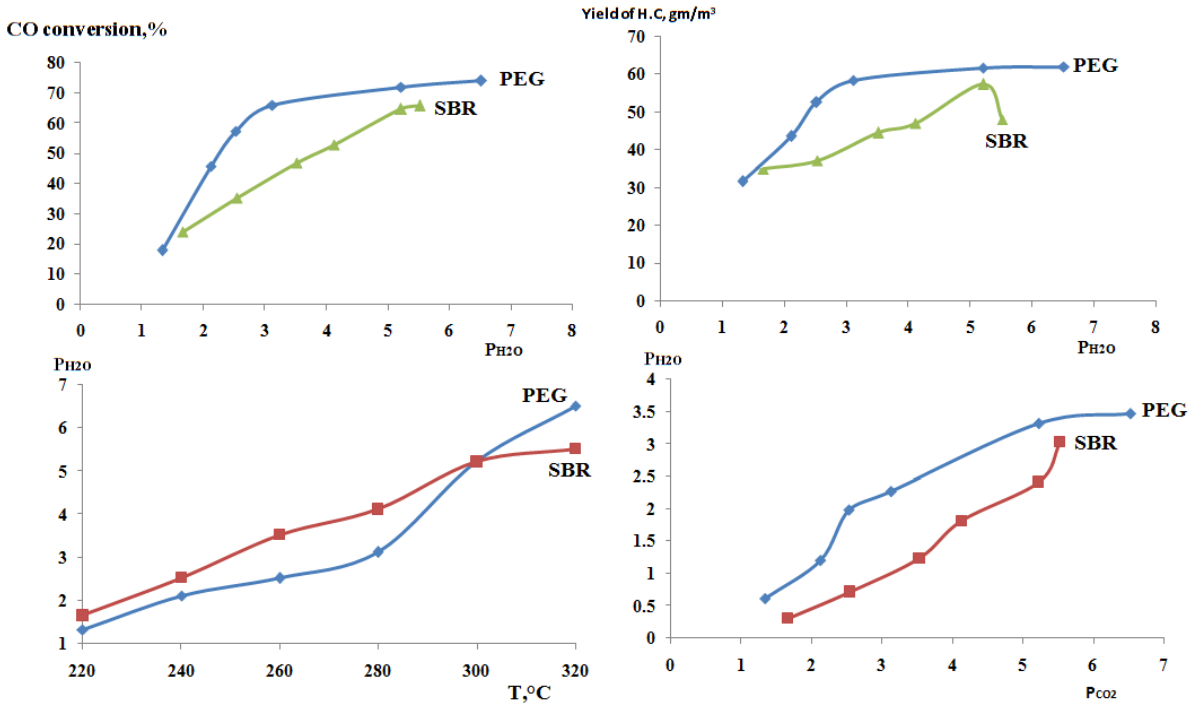

Fig. 3 Dependences of the H_2O partial pressure with: CO conversion, yield of liquid hydrocarbons, Temperature and CO_2 partial pressure

D.Kinetic Study

For iron catalysts the FT reaction rate increases with H_2 partial pressure and decreases with partial pressure of water.A study in 1972, Dry and co-workers reported that water is believed to bethe primary byproduct of the FT synthesis and CO_2 is produced by the WGS.

$$CO + H_2O \longrightarrow H_2 + CO_2$$

Here, we have applied the kinetic equations for the FT reactions,[15] and usetheobtained results to determine the best equations and whichone can describe the experimental data for each nanocatalyst. The most common four mechanisms and their corresponding equations were used to calculate the rate of the FT reaction that based on the rate of adsorption of CO as a predominant adsorbent on the nano-iron

surface.[16]The models that are illustrated in the table 3 are based on predicted elementary stages of the Fischer-Tropsch reactions, carbide mechanism, enolic mechanism, combination enol-carbide and parallel enol-carbide.

Table 3 Elementary reaction mechanism set for FTS

a) Carbide mechanism

$$CO + 2s \leftrightarrow Cs + Os$$
$$H_2 + 2s \leftrightarrow 2Hs$$
$$Cs + Hs \leftrightarrow HCs + s$$
$$HCs + Hs \leftrightarrow H_2Cs + s$$
$$Os + Hs \rightarrow HOs + s$$
$$HOs + Hs \rightarrow H_2O + 2s$$

b) Enolic mechanism

$$CO + s \leftrightarrow Cos$$
$$COs + H_2 \leftrightarrow H_2COs$$
$$H_2COs + H_2 \leftrightarrow CH_2s + H_2O$$
$$H_2 + 2s \leftrightarrow 2Hs$$

c) Combination enol-carbide

$$CO + s \leftrightarrow COs$$
$$H_2 + 2s \leftrightarrow 2Hs$$
$$COs + Hs \leftrightarrow HCOs + s$$
$$HCOs + Hs \leftrightarrow Cs + H_2O + s$$
$$Cs + Hs \leftrightarrow CHs + s$$
$$CHs + Hs \leftrightarrow CH_2s + s$$
$$Os + Hs \rightarrow HOs + s$$
$$HOs + Hs \rightarrow H_2O + 2s$$

d) Parallel enol carbide

$$CO + s \leftrightarrow COs$$
$$H_2 + 2s \leftrightarrow 2Hs$$
$$COs + Hs \leftrightarrow HCOs + s$$
$$HCOs + Hs \rightarrow CHs + OHs$$
$$COs + s \rightarrow Cs + Os$$
$$Cs + Hs \leftrightarrow CHs + s$$
$$CHs + Hs \leftrightarrow CH_2s + s$$
$$Os + Hs \rightarrow HOs + s$$
$$HOs + Hs \rightarrow H_2O + 2s$$

Table 4 Experimental data for various catalytic systems Fe – paraffin – polymer

nanocatalyst	nm	T,K	P_{H2O}	P_{H2}	P_{CO2}	P_{CO}	K_{H2O}	R_{CO},mol.g^{-1} cat.min^{-1}
		473	1.3361	9.4	0.618	8.89	0.0530	0.008585
	9% at181	493	2.122	8.45	1.21	8.87	0.0544	0.022107
Fe-P/PEG	91%at 655	513	2.526	7.81	1.992	7.88	0.0553	0.027703
		533	3.123	6.12	2.278	6.41	0.0651	0.031927
		553	5.221	4.34	3.316	5.11	0.0704	0.034745
		573	6.521	3.11	3.468	3.11	0.0886	0.035783
		473	1.661	8.4	0.312	8.34	0.0513	0.0115441
		493	2.542	7.45	0.723	8.12	0.0583	0.0169715
Fe-P/SBR	19% at 171	513	3.526	6.81	1.245	7.76	0.0618	0.0226571
	81%at 664	533	4.123	5.12	1.821	7.42	0.0689	0.0255366
		553	5.221	3.34	2.417	6.07	0.0747	0.0312069
		573	5.521	2.11	3.031	4.25	0.0809	0.0317598

The results in the Table 4 show, the R_{CO}dependencies on temperature reactor for two catalytic systems,and these results are match other data researchers.[15-16]

To calculate consumption rate of CO, equation used (Zennaro et al., 2000; Levenspiel, 1999)

$$-R_{CO} = \frac{X_{CO}F^{\circ}_{CO}}{W_{cat}}$$

F^0CO : Inlet Molar Flow of CO (mol.min-1).

X_{CO} : Conversion of CO, %.

W_{cat} : Wight of catalyst

The Rate constants are calculated according to the following representation:

$$K_{obs.} = A{\cdot}exp(-Ea/RT)$$

Fromthe reactionmechanismequilibriums above, it was observedthat stages 3 are the limited step. E_a is the activation energy that contains energy limited stage $E_{a,lim}$ and the change in enthalpy of CO adsorption:

$$E_a = E_{a,lim.} + \Delta H_{ads}$$

In this case, the Arrhenius equation takes the form:

$$K_{obs.} = A{\cdot}e^{[-(Ea,lim. + \Delta Hads.)/RT]}$$

For the adsorption coefficients, we can write:

$$a = a_0{\cdot}e^{(-\Delta Hads.)/RT}$$

ΔH_{ads} is the heat of CO adsorption on the surface iron, it is known in the literature[14]asconstant value and equal (-47 kJ/ mol).The value of a_0 is $8.3*10^{-8}$mmol/ g atm. Therefore, the mechanisms that we have used are the heat of CO adsorption on the surface ironasconstant value.The value of $a_0$is varied and theminimum limitwas used to obtain the function lnYvs 1/ T for all mechanisms see (Figurer 4).

The listed results in figurer 4 that obtained using kinetic equation for the four mechanisms, shows that there are only two of them; Enolic mechanism and Parallel enol carbideare suitable for our experiments. Out of these two mechanisms, Parallel enol carbide was better, since it matches Arrhenius equation and the activation energy is 70.35 and 82.46 KJ/mol for PEG and SBR respectively. The following equation was used for our calculation:

$$-R_{CO} = K_{obs.}P_{CO}P_{H2} + FP_{CO} / (1 + aP_{CO})^2$$

a) Carbide mechanism

Rate equation:

$$-R_{CO} = K_{ods}P_{CO}^{0.5} / 1 + a\,P_{CO}^{0.5}$$

Substituted the value K_{obs} and a_0 in all equations follows:

$$-R_{CO} = K_{ods}P_{CO}^{0.5} / 1 + a\,P_{CO}^{0.5}$$

$$P_{CO}^{0.5}P_{H2} / R_{CO} = 1/K_{obs}. + a_0/ K_{obs}\,P_{CO}$$

$$P_{CO}^{0.5}P_{H2} / R_{CO} = 1/[A\cdot e^{[-(Ea,lim. + \Delta Hads.)/RT]}] + a_0/A\cdot e^{[-(Ea,lim. + \Delta Hads.)/RT]}P_{CO}^{0.5}$$

After simplification we get:

$$[e^{(\Delta Hads.)/RT} + a_0 P_{CO}^{0.5}] / (P_{CO}^{0.5}P_{H2} / R_{CO}) = A\cdot e^{[-(Ea,lim..)/RT]}$$

$$Y = [e^{(\Delta Hads.)/RT} + a_0\,P_{CO}^{0.5}] / (P_{CO}^{0.5}P_{H2} / R_{CO})$$

$$Y = A\cdot e^{[-(Ea,lim..)/RT]}$$

$$ln\ Y = ln\ A - (E_{a,lim}/R)\ .\ 1/T$$

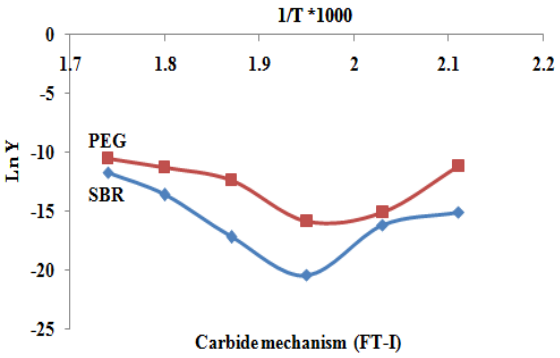

b) Enolic mechanism

Rate equation:

$$-R_{CO} = K_{obs}.P_{CO} / 1 + aP_{CO}$$

$$P_{CO}/ R_{CO} = 1/K_{obs}. + a_0 / K_{obs}\,P_{CO}$$

$$P_{CO}/ r_{CO} = 1/[A\cdot e^{[-(Ea,lim. + \Delta Hads.)/RT]}] + a_0 /A\cdot e^{[-(Ea,lim. + \Delta Hads.)/RT]}P_{CO}$$

After simplification we get:

$$[e^{(\Delta Hads.)/RT} + a_0 P_{CO}] / (P_{CO} / R_{CO}) = A\cdot e^{[-(Ea,lim..)/RT]}$$

$$Y = [e^{(\Delta Hads.)/RT} + a_0 P_{CO}] / (P_{CO} / R_{CO})$$

$$Y = A\cdot e^{[-(Ea,lim..)/RT]}$$

$$ln\ Y = ln\ A - (E_{a,lim}/R)\ .\ 1/T$$

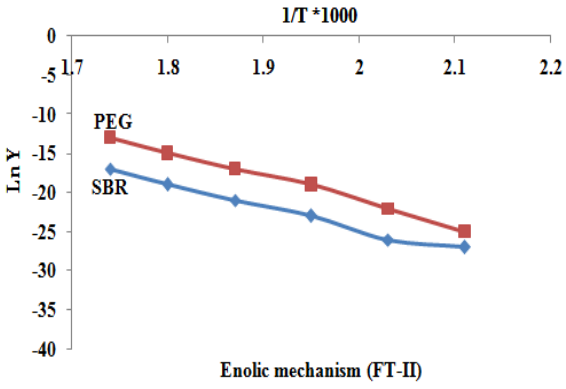

ΔH_{ads} = -47 kJ/ mol , a_0 = 8.3*10^{-8}mmol/ g ·atm

For *Fe-P/ PEG*

$E_{a,lim}$ =122.312 kJ/ mol , $E_{a,total}$ =75.312kJ/mol and A = .1.67*10^{-5}

For *Fe-P/ SBR*

$E_{a,lim}$ =131.840 kJ/ mol, $E_{a,total}$ = 84.84 kJ/ mol

A = 1.125*10^{-7}.

c) combination enol-carbide

Rate equation:

$$-R_{CO} = K_{obs}.P_{H2} / (1 + aP_{CO})^2$$

$$P_{H2}/ R_{CO} = 1/K_{obs}. + (a_0/ K_{obs})^2 P_{CO}^2$$

$$P_{H2}/ R_{CO} = 1/[A\cdot e^{[-(Ea,lim. + \Delta Hads.)/RT]}] + (a_0 /A\cdot e^{[-(Ea,lim. + \Delta Hads.)/RT]})^2 P_{CO}^2$$

After simplification we get:

$$[e^{(\Delta Hads.)/RT} + a_0^2 P_{CO}^2] / (P_{H2} / R_{CO}) = A\cdot e^{[-(Ea,lim..)/RT]}$$

$$\boldsymbol{Y} = [e^{(\Delta Hads.)/RT} + a_0^2 P_{CO}^2] / (P_{H2} / R_{CO})$$

$$Y = A\cdot e^{[-(Ea,lim..)/RT]}$$

$$ln\ Y = ln\ A - (E_{a,lim}/R)\ .\ 1/T$$

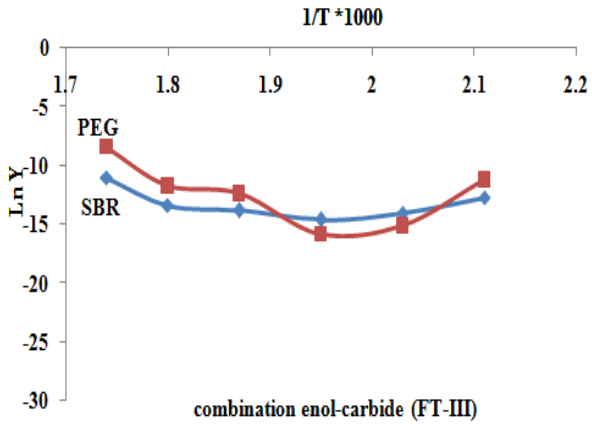

d) Parallel enol carbide

Rate equation:

$$-R_{CO} = K_{obs}.P_{CO}P_{H2} + FP_{CO} / (1 + aP_{CO})^2$$

$$P_{CO}P_{H2} + FP_{CO}/ R_{CO} = 1/K_{obs}. + (a_0 / K_{obs})^2 P_{CO}^2$$

$$P_{CO}P_{H2} + FP_{CO}/ R_{CO} = 1/[A\cdot e^{[-(Ea,lim. + \Delta Hads.)/RT]}] + (a_0 /A\cdot e^{[-(Ea,lim. + \Delta Hads.)/RT]})^2 P_{CO}^2$$

After simplification we get:

$$[e^{(\Delta Hads.)/RT} + a_0^2 P_{CO}^2] / P_{CO}P_{H2} + FP_{CO}/ R_{CO} = A\cdot e^{[-(Ea,lim..)/RT]}$$

$$\boldsymbol{Y} = [e^{(\Delta Hads.)/RT} + a_0^2 P_{CO}^2] / (P_{H2} / R_{CO})$$

$$Y = A\cdot e^{[-(Ea,lim..)/RT}$$

$$ln\ Y = ln\ A - (E_{a,lim}/R)\ .\ 1/T$$

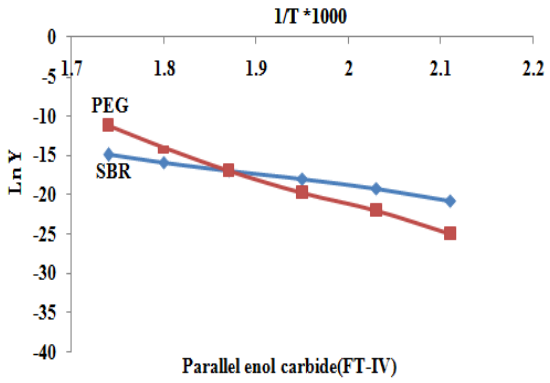

ΔH_{ads}=-47 kJ/ mol, a0 = 8.3*10-8 mmol/ g atm

For *Fe-P/ PEG*

$E_{a,lim}$ = 117.35kJ/ mol, $E_{a,total}$ =70.35kJ/ mol

A = $4.539*10^{-5}$.

For *Fe-P/ SBR*

$E_{a,lim}$ = 129.46kJ/ mol, $E_{a,total}$ =82.46kJ/ mol

A = $3.059*10^{-7}$.

Fig. 4 Dependences of the function lnYvs 1 / T: a) Carbide mechanism; b) Enolic mechanism; c) combination enol-carbide and d) Parallel enol carbide.

Conclusions

Thecalculation that obtained from kinetic equations for the FT reactions showed that the models enolic (b) and parallel enol-carbide(d) mechanisms were the more suitablefor our study. The activation energy for various kinetic expressions was in the range of 70–84 kJ/mol. The iron -paraffin/ polymer as nanocatalyst in the case PEG gave the highest result for the CO conversion and yield liquid hydrocarbons. Finally, the ratio weight content that obtained from small nanoparticles with PEG was 9%less than the one with

SBR19%.For both nanocatalysts the weight content ratio in the large nanoparticles was dominant. Finally, the XRD showed that the iron in the active nanocatalysts is existing in the form of Fe_3O_4.

Acknowledgments

I would like to acknowledge the A. V. Topchiev Institute of Petrochemical Synthesis, Russian Academy of Sciences for providing all the instruments for our work, which was supported by the President of Russian the Federation. Many thanks to A.V. Krylov,O. S. Dement'eva, M.V. Kulikova, V.R. Flid and S. N.Khadzhiev, for their help in our work.

References

[1] Kulikova, M. V.; Al Khazraji, A. H.; Dement'eva, O. S.; Ivantsov, M. I.; Flid,V.R.; Khadzhiev, S. N. Petroleum Chemistry. **2015**, 55, 537–541.
[2] Al-Khazraji A.H.; Tsvetkov V.B.; Dementyeva O.S.; Kulikova M.V.; Flid V.R.; Khadzhiev S.N.12th European Congress on Catalysis – EuropaCat-XII, Kazan, Russia, 30 August – 4 September, **2015**, 1373-1374.
[3] Kulikova , M. V.; Ivantsov , M. I.; Efimov, M. N.; Zemtsov, L. M.; Chernavskii, P. A.; Karpacheva, G. P.; Khadzhiev, S. N. Eur. Chem. Bull, **2015** , 4(4), 181-185.
[4] AlKhazraji, A.H.; Krylov, A.V.; Kulikova, M.V.; Flid, V. R.; Tkachenko, O. Yu. Fine Chemical Technologies. **2016**, 11, 70-77.
[5] Alkhazraji, A.H.; Dementyeva, O.S.; Pastukhova, Z.; Kulikova, M.V.; Flid, V.R. Journal of Physics: Conf. Series ; **2018**, 1032 ,1-10, 012065.
[6] Ott, L. S.; Finke, R. G. Chem. Mater. **2008**, 20 (7), 2592–2601.
[7] Besson, C.; Finney, E. E.; Finke, R. G. Chem. Mater. **2005**, 17 (20), 4925–4938.
[8] Quesada, M. C.; Yarulin, A.; Jin, M.; Xia, Y.; Minsker, L. K. J. Am. Chem. Soc.**2011**, 133 (32), 12787–12794.
[9] Perego, C.; Bortolo, R.; Zennaro, R. Catalysis Today. **2009**, 142, 9-16.
[10] Munnik, P.; Jongh, P. E.de.; Jong, K. P. de . J. Am. Chem. Soc. **2014**, 136 (20), 7333–7340.
[11] Botes, G. F.Ind. Eng. Chem. Res, **2009**, 48 (4), 1859–1865.
[12] Mohajeri, A.; Zamani, Y.; Shirazi, L. Journal of Nanoanalysis, **2014**, 2, 58-64.
[13] Pirola, C.; Di Fronzo, A.; Galli, F.; Bianchi, L. Claudia.; Comazzi, A.; Manenti, F. CHEMICAL ENGINEERING TRANSACTIONS. **2014**, 37, 595-600.
[14] Atashi, H.; Fazlollahi, F.; Sarkarizi, M.; Mirzaei, A.; Shahrasb, M. NTERNATIONAL JOURNAL OF CHEMICAL REACTOR ENGINEERING. **2011**, 9, 1–31.
[15] Mirzaei, A.;Arsalanfar, M.;Ebrahimzadeh, F.;Atashi, H.;Moghaddam, S. Phys.Chem. Res. **2013**, 1. 69–80.
[16] Nakgul, A.;Narataruksa, Ph.;Tungkamani, S.;Phongaksorn, M. Catalyst. **2012**, 43, P, 87–92.